

Multi-material distributed recycling via Material Extrusion: rHDPE and rPET case of study

Catalina Suescun Gonzalez¹²³, Fabio A. Cruz Sanchez¹, Hakim Boudaoud¹, Cécile Nouvel², Joshua Pearce³

¹Université de Lorraine – ERPI – F-54000, Nancy, France

²Université de Lorraine, CNRS, LRGP, F-54000 Nancy, France

³Western University, Department of Electrical & Computer Engineering, Canada, London

Abstract

The high volume of plastic waste and the extremely low recycling rate have created a serious challenge worldwide. Local distributed recycling coupled with additive manufacturing (DRAM) offers a solution by economically incentivizing local recycling. One DRAM technology capable of processing large quantities of plastic waste is fused granular fabrication (FGF), where solid shredded plastic waste can be reused directly as 3D printing feedstock. This study presents an experimental assessment of multi-material recycling printability using two of the most common thermoplastics in the beverage industry, polyethylene terephthalate (PET) and high-density polyethylene (HDPE), and the feasibility of mixing PET and HDPE to be used as a feedstock material for large-scale 3-D printing. After the material collection, shredding, and cleaning, the characterization and optimization of parameters for 3D printing were performed. Results showed the feasibility of printing a large object from rPET/rHDPE flakes, reducing the production cost by up to 88%.

Acronyms

Acronym	Definition
ABS	Acrylonitrile Butadiene Styrene
AM	Additive Manufacturing
DRAM	Distributed recycling via additive manufacturing
DSC	Differential scanning calorimetry
FDM	Fused deposition modeling
FFF	Fused filament fabrication
FGF	Fused granular fabrication
FPF	Fused particle fabrication
FTIR	Fourier-transform infrared spectroscopy
HDPE	High-density polyethylene
MFI	Melt flow index
PC	Polycarbonate
PET	Poly(ethylene terephthalate)
PLA	Poly(lactic acid)
PP	Polypropylene
PSO	Particle swarm optimization
PS	Polystyrene
SEBS	Poly (styrene-block-ethene-co-butene-block-styrene)
Tg	Glass temperature
pBC	Printed Bottle-Cap
rHDPE	Recycled High-density Polyethylene
rPET90//rHDPE10	Recycled Bottle-Cap (Cristaline bottle shredded without separation)
rPET	Recycled Poly(ethylene) terephthalate
vPET	Virgin or commercial Poly(ethylene terephthalate)

Introduction

- ¹ The disposal of plastic waste is one of the most challenging current environmental concerns
² given its systemic complexity ([Evode et al., 2021](#)). The mass of micro- / meso- plastics in
³ the oceans is expected to exceed the mass of the global stock of fish by 2050 ([MacArthur, 2017](#)). More critically, the global annual plastic production is expected to reach 1100 metric
⁵ tons by the same year ([Geyer, 2020](#)). Societal awareness of plastic recycling has received
⁶ substantial attention from scientists, policymakers, and the general public ([Soares et al., 2021](#)). Unfortunately, the statistical analysis of the centralized recycling process proves that
⁷ it has been largely ineffective ([Siltaloppi and Jähi, 2021](#)) with only 9% of the plastic produced
⁸ since 1950 being recycled from the total stock ([Geyer et al., 2017](#)). Therefore, it remains an
⁹ open challenge to identify alternatives to valorize discarded plastic material.
¹⁰

11 Distributed recycling and additive manufacturing (DRAM) is an innovative technical ap-
12 proach to recycling plastic waste (Cruz Sanchez et al., 2020; Dertinger et al., 2020). DRAM
13 was initially implemented using recyclebots, which are waste plastic extruders that produce
14 filament for conventional fused filament-based 3-D printers (Baechler et al., 2013; Woern et
15 al., 2018; Zhong and Pearce, 2018). Previous studies have shown that distributed recycling
16 aligns with the circular economy paradigm (Despeisse et al., 2017; Ford and Despeisse, 2016).
17 This approach allows consumers to directly recycle their own waste into consumer products
18 using open-source designs, ranging from toys for children (Petersen et al., 2017) to adaptive
19 aids for individuals with arthritis (Gallup et al., 2018). Distributed manufacturing is now
20 widely adopted (Pearce and Qian, 2022). In this way, DRAM-based recycling operates within
21 a closed-loop supply chain network (Santander et al., 2020). The primary goal of this type of
22 recycling is to reduce the environmental impact by minimizing the transportation from the
23 waste source to recycling facilities (Kreiger et al., 2014). In that sense, it aims to propose
24 innovative closed-loop strategies that utilize waste materials as raw resources (Romani et al.,
25 2021).

26 Fused filament fabrication (FFF, which is also known as Fused Deposition Modelling –FDM©–
27) is the most widespread and established extrusion-based AM technology. It has gained
28 popularity due to the open-source proliferation from the self-replicating rapid prototyper
29 (RepRap) project (Bowyer, 2014; Jones et al., 2011; Sells et al., 2009). FFF is favored for
30 its simplicity, versatility, low cost, and ability to construct complex geometric objects in the
31 industrial and prosumer domains (Romani et al., 2021). Indeed, the open-source approach
32 for 3-D printing has facilitated significant advancements in manufacturing and prototyping
33 adding value to the recycled material (Cruz Sanchez et al., 2020). Efforts are being made
34 to identify sustainable feedstocks for 3-D printing Pakkanen et al. (2017a). Several studies
35 have expanded the range of recycled filament materials including PLA (Anderson, 2017;
36 Cruz Sanchez et al., 2017), ABS (Mohammed et al., 2017b, 2017a), PET (Vaucher et al.,
37 2022; Zander et al., 2018), HDPE (Baechler et al., 2013; Chong et al., 2017; Mohammed
38 et al., 2017b), and PC (Gaikwad et al., 2018). In fact, Kreiger et al. (2014) conducted a

39 comparative life cycle assessment in a low-density population case study in Michigan (USA)
40 and estimated that a distributed approach could save approximately 100 billion MJ of energy
41 per year from the recycling of 984 million pounds of HDPE. There is substantial evidence
42 that DRAM can contribute to reducing energy consumption and greenhouse emissions in
43 manufacturing processes.

44 Most DRAM studies have used mono-materials for the fabrication of feedstock for FFF. There
45 are, however, several examples of mixed materials including wood waste and recycled plastic
46 ([Löschke et al., 2019](#); [Pringle et al., 2018](#)) and textile fibers and recycled plastic ([Carrete et al.,](#)
47 [2021](#)). Recently, Zander et al. ([2019](#)) reported the manufacturing of composite filament from
48 recycled PET/PP and PS/PP blending through a compatibilizer copolymer such as SEBS.
49 Their results revealed the technical printability of polypropylene blend composite filaments
50 from a thermo-mechanical characterization perspective. Increasing the performance window
51 of blending materials by compatibilization which could be a relevant path for recycling plastics
52 at a local level and in isolated areas contexts (e.g. during humanitarian crises ([Corsini et](#)
53 [al., 2022](#); [Lipsky et al., 2019](#); [Savonen et al., 2018](#)), supply chain disruptions ([Attaran,](#)
54 [2020](#); [Choong et al., 2020](#) ; [Novak and Loy, 2020](#); [Salmi et al., 2020](#)) and/or isolated
55 off-grid situations using solar-powered 3-D printers ([Gwamuri et al., 2016](#); [King et al., 2014](#);
56 [Mohammed et al., 2018](#); [Wong, 2015](#))). Likewise, Vaucher et al. ([2022](#)) studied the evaluation
57 of the microstructure, mechanical performance, and printing quality of filaments made from
58 rPET and rHDPE varying the wt% of HDPE material from 0 to 10%. They confirmed the
59 increase in Young's modulus from 1.7 GPa of the pure PET to 2.1 GPa for all the HDPE
60 concentrations. Additionally, the maximum stress of the bends was augmented with high
61 HDPE concentrations. Values were lower than virgin PET filament, yet similar to commercial
62 recycle ones. The addition of rHDPE at higher levels, however, helped to meet the brittle-
63 ductile transition in 15% despite the low interfacial tension of both polymers, allowing the
64 printing of quality parts.

65 While former studies have proven successful in FFF, a new approach to DRAM is fused
66 granular fabrication (FGF) or fused particle fabrication (FPF), where the material-extrusion

67 AM systems print directly from pellets, granules, flakes, shreds or grinder material (Fontana
68 et al., 2022; Woern et al., 2018). In the context of recycling, this could reduce the number
69 of melt/extrusion cycles that degrade the material needed in the filament fabrication process
70 (Cruz Sanchez et al., 2017). The FGF technique opens up the potential to use recycled
71 materials as well as print large-scale objects either with a conventional cartesian 3-D printer
72 (Woern et al., 2018), delta 3-D printer (Grassi et al., 2019) or hangprinter (Petsiuk et al.,
73 2022; Rattan et al., 2023). Research groups have corroborated that plastic waste can be
74 used as feedstock materials for FGF/FPF. Alexandre et al. (2020) assessed the technical and
75 economical dimensions of virgin and shredded PLA printed in a self-modified FGF machine
76 and compared it with FFF. The investigation showed that the use of FGF reduced printing
77 costs, time and its mechanical performance was comparable to that obtained using the tra-
78 ditional FFF technique. Likewise, Woern et al. (2018) found comparable properties between
79 PLA, ABS, PP, and PET recycled and virgin materials. Later publications demonstrated
80 the technical and economic feasibility through the printing of complex objects validating the
81 possibility of recycling plastic with FGF in both conventional and common FFF materials
82 (Byard et al., 2019), but also recycling PC (Reich et al., 2019) and rPET (Little et al., 2020).
83 Few researchers, however, have addressed the problem of directly printing recycled multi-
84 materials, which might be a key step forward needed to facilitate the ease of sorting and
85 recycling post-consumer plastic waste materials.

86 This study explores the potential of direct 3-D printing of two immiscible polymers commonly
87 used in the beverage sector through a distributed recycling process for its easy implemen-
88 tation operation at the local level. To demonstrate the feasibility of the process, the most
89 commonly used plastic for bottled water in France, which consists of roughly 90% PET (body
90 of the bottle) and 10% HDPE (cap) now referred to as *rPET90//rHDPE10*, is used as a test
91 material. The experimental process of collection, characterization, and printing of the recy-
92 cled material is described, and the results are discussed in the context of widespread DRAM
93 adoption at the community-based level.

94 Materials and Methods

95 The methodology presented in Figure 1 outlines the approach adopted to develop the study.
96 The three stages, namely *Material obtention*, *Printing process*, and *Evaluation* were thor-
97oughly studied to control the major process steps and the technical characterization methods.
98 In the following subsections, each step is explained.

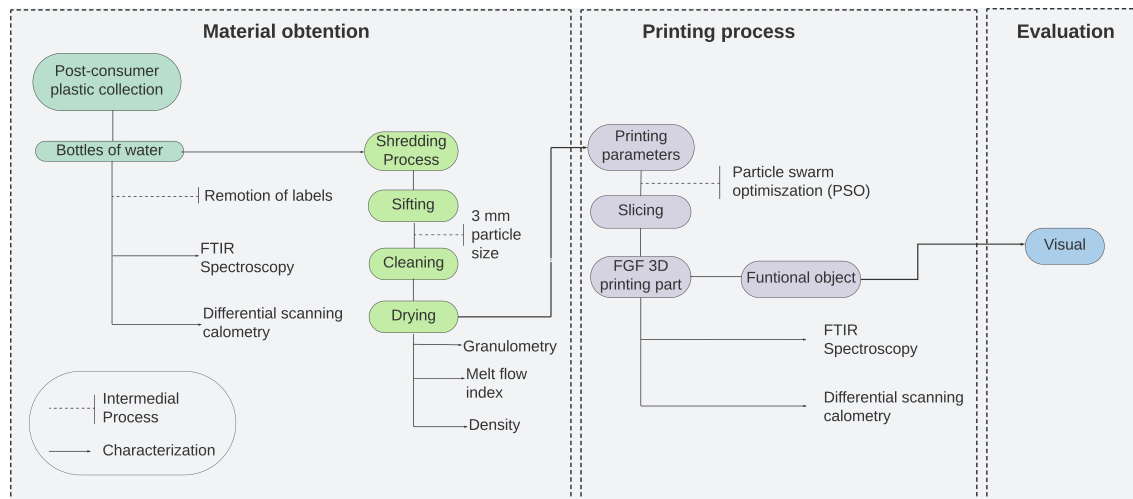


Figure 1: Global framework of the study

99 Raw material obtention

100 The goal of the material stage is to collect and prepare post-consumer plastic sources. In
101 this study, water bottles coming from the French brand Cristaline[©] were used as feedstock.
102 The process steps used are shown in Figure 2 a/b. Post-consumer bottles were collected
103 from receptacles placed in partnership schools in Lorraine, France. To convert the complete
104 water bottles including their caps into 3DP feedstock material, the labels were removed before
105 shredding in a cutting mill (Retsch MS300) using a 3 mm grid. After shredding, the obtained
106 flakes were sifted with a 1.5 mm, 3 mm, and 5 mm sifters for further analysis. Next, the
107 flakes were cleaned with hot water in an ultrasonic machine at 60°C for 1 hour to remove
108 contaminants. Lastly, they were dried in a conventional oven overnight at 80°C (Taghavi
109 et al., 2018; Van de Voorde et al., 2022) to avoid degradation of the material. Washing

110 conditions were the same for all the samples; therefore, the effect of contaminants was not
111 considered. The resultant material is shown in Fig 2.c.



Figure 2: Process steps to prepare the collected material

112 The material composition was calculated as a function of the mass of the bottles and caps
113 separately. The percentage (%) of bottle-cap was found to be ~90%rPET (bottle) and ~10%
114 rHDPE (cap). The complete bottle was shredded without separation of both materials thus
115 this percentage is constant for all the samples.

116 Material preparation and characterization

117 Material particle size analysis -Granulometry-

118 In order to ensure the particle size suitable for printing, the granulate particles were char-
119 acterized using the open-source ImageJ software ([ImageJ, 2023](#)). The size characteristics of
120 the particles were evaluated in four different samples: vPET (used as a reference) and the
121 raw material sifted into three different sizes: 1.5 mm, 3 mm, and 5 mm.

122 Fourier-transform infrared spectroscopy –FTIR-

123 FTIR spectroscopy was conducted to determine the composition of the bottle and identify
124 any impurities, plasticizers, or additives. The analysis involving testing separate samples
125 of rPET and rHDPE. Additionally, a printed sample of both materials was examined to
126 identify any potential chemical bonding. Each sample was measured at two different points,
127 with three measurements taken at each point. The resulting curves were then normalized
128 and analyzed using Origin Pro 8. The Fourier transform infrared spectra were recorded in
129 the range of 4000 cm^{-1} to 375 cm^{-1} with a resolution of 4 cm^{-1} using a Bruker IFS 66V
130 spectrophotometer.

131 Differential scanning calorimetry –DSC-

132 Differential scanning calorimetry analysis was performed using a DSC-1 Mettler Toledo with
133 STArE software operating under nitrogen atmosphere at heating rate and cooling rate of
134 $10\text{ }^{\circ}\text{C/min}$. The samples investigated were rPET, rHDPE, and rPET90//rHDPE10. Three
135 cycles were conducted: the first involved heating from 20°C to 270°C , cooling to 20°C and
136 reheating to 270°C . The rHDPE sample was analyzed using similar cycles but with the
137 maximum temperature set at 250°C and the blend was tested at temperatures ranging from
138 -20 to 270°C . The glass transition temperature (T_g) of rPET was determined during the first
139 heating cycle, while the T_g of rPET90//rHDPE10 was determined during the second heating
140 cycle, along with the melting point of all materials. The crystallization temperature (T_c) was
141 determined during the cooling cycle for each material. The degree of crystallinity (X_c) was
142 calculated from the second cycle for recycled materials and the first cycle for the blend, as
143 expressed in equation (1) ([Pan et al., 2020](#); [Taghavi et al., 2018](#)):

$$X_c(\%) = \frac{\Delta H_m}{w \cdot \Delta H_m^\circ} \quad (1)$$

144 Where, ΔH_m is the latent heat of melt, w is the weight percentage of polymer in the blend,
145 and ΔH_m° is the reference heat of 100% crystalline PET (140 J/g) and HDPE (293 J/g),

¹⁴⁶ respectively, provided in the literature ([Kratofil et al., 2006; Pan et al., 2020](#)).

¹⁴⁷ Melt Flow Index –MFI-

¹⁴⁸ The melt-flow index (MFI) of rPET90//rHDPE10 flakes was determined using an Instron
¹⁴⁹ CEAST MF20. The analysis was performed using three samples of ~5 g at a temperature of
¹⁵⁰ 255 °C with a 2.16 kg weight following the ASTM D1238 standard. The process was repeated
¹⁵¹ three times. The average value of the three results was reported in units of *gr/10 × min.*

¹⁵² Density

¹⁵³ The material's density was calculated as follows: first, the volume was found by mea-
¹⁵⁴ suring the dimensions of a solid 50x50x50 mm cubic geometry fabricated by injecting
¹⁵⁵ rPET90//rHDPE10 flakes into a square mold with a known volume using an open-source
¹⁵⁶ desktop injection machine(Holipress, Holimaker, France). Then, the model was weighed, and
¹⁵⁷ the mass was obtained. Finally, the density was calculated as expressed in [Equation 2](#). To
¹⁵⁸ ensure the accuracy of the test it was performed twice and the average value was reported
¹⁵⁹ in *g/cm³*.

$$\rho = V/m \quad \left[\frac{g}{cm^3} \right] \quad (2)$$

¹⁶⁰ Where, ρ is the density, V is the volume, and m the mass.

¹⁶¹ Afterwards, experimental results were compared with the theoretical blend density which
¹⁶² could be calculated by [Equation 3](#).

$$\rho_{12} = \frac{1}{\frac{W_1}{\rho_1} + \frac{W_2}{\rho_2}} \quad \left[\frac{g}{cm^3} \right] \quad (3)$$

¹⁶³ Where, ρ_{12} is the density of the blend, W_1 and W_2 , the weight fractions of each polymer, ρ_1
¹⁶⁴ and ρ_2 , the theoretical density of each polymer for PET (1.38 *g/cm³*) and HDPE 0.93 to
¹⁶⁵ 0.97 *g/cm³* ([Jonathan GUIDIGO1 et al., 2017](#)).

₁₆₆ **Printing process**

₁₆₇ **Establishing optimal parameters**

₁₆₈ Establishing the optimal combinations of parameters is essential for improve the quality
₁₆₉ and mechanical properties of printed parts ([Jaisingh Sheoran and Kumar, 2020](#)). Accord-
₁₇₀ ing to Oberloier et al. ([2022a](#)), particle swarm optimization (PSO) is an accurate and
₁₇₁ time-effective method for achiving this goal. To optimize the 3-D printing parameters for
₁₇₂ the rPET90//rHDPE10 material in the GigabotX we utilized the open-source PSO Experi-
₁₇₃ menter platform which is available for Linux. The methodology developed by Oberloier et al.
₁₇₄ ([2022a](#)) was followed during the optimization. For benchmarking purposes, three artifacts
₁₇₅ were printed: a line, a plane, and a cube. These artifacts were modeled in CAD software
₁₇₆ Onshape CAD v1.150 and sliced using Prusaslicer v2.52.0. Figure 3 presents the geometry
₁₇₇ models and dimensions of the artifacts.

Geometry	Lenght (mm)	width (mm)	height (mm)
Line	200	2	1
Plane	100	100	1
Cube	40	40	40

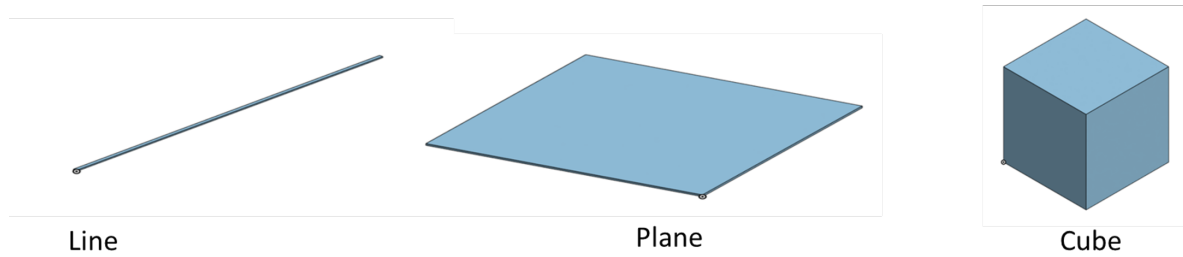


Figure 3: Dimensions and CAD models of the geometries used for parameters optimization.

₁₇₈ Four parameters were assessed: 1) nozzle temperature, 2) bed temperature, 3) printing speed
₁₇₉ and 4) extrusion multiplier ([Oberloier et al., 2022b](#)). The initial parameters for the line are
₁₈₀ presented in Table 1a while additional parameters were obtained from preliminary experi-
₁₈₁ mental work shown in Table 1.b. Finally, the PSO tuning parameters were found in the
₁₈₂ previous PSO work ([Oberloier et al., 2022a](#)) Table 1.c.

Table 1: table 1

(a) Line optimization initial parameters

Variable	Min	Max	Guess	True/False	Description
T1	255	270	260	TRUE	Temperature Zone 1 on GigabotX
Tb	80	90	85	TRUE	Bed temperature
Ps	10	25	15	TRUE	Printing Speed
E	0.5	2	1	FALSE	Extrusion Multiplier

(b) Fixed parameters to perform printing parameters optimization based on PSO

Parameters	Value	Units
Layer height	0.5	mm
Width	2	mm
T2	230	°C
T3	220	°C
Cooling	0	%
Infill density	2	%

(c) Recommended parameters for PSO tuning

Variable	Value	Description
Kv	0.5	The emphasis given to the velocity component
Kp	1.0	The emphasis given to a particle's personal best position
Kg	2.0	The emphasis given to the swarm's group's best position

183 Fused Granular Fabrication –FGF–

184 To print the obtained raw material, a modified open-source printer with three heat zones
 185 (Gigabot XL re:3D, Houston, TX, USA) was utilized as illustrated in Figure 4. The machine
 186 is a single screw extrusion-based 3-D printer capable of direct printing pellets, flakes, or
 187 granules, with a nozzle size of 1.75 mm. For this study, a chair was printed to evaluate the
 188 material's ability to be 3-D printed and the printer's capability to produce large objects like
 189 furniture. The ideal parameters determined for the cube geometry were employed to print
 190 the final part.

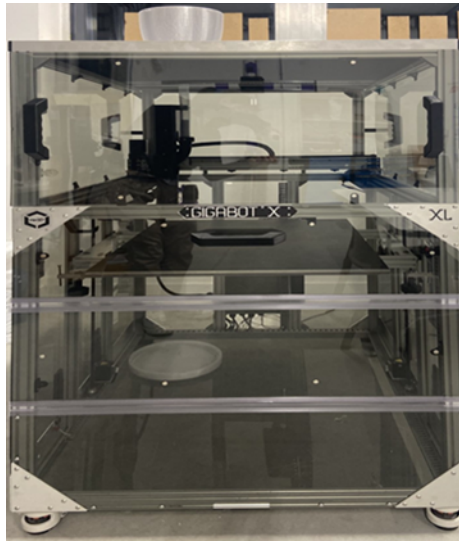


Figure 4: Fused granular fabrication printer Gigabot

¹⁹¹ Results and discussion

¹⁹² Material characterization

¹⁹³ Both the polymeric components of the bottle and the blend were characterized and analyzed
¹⁹⁴ to determine their properties using different methods as described in the preceding section.

¹⁹⁵ Material particle size analysis (granulometry)

¹⁹⁶ Previous studies demonstrated that particles with areas smaller than 22 mm^2 were optimal
¹⁹⁷ for printing without experiencing jamming or under-extrusion problems ([Woern et al., 2018](#)).
¹⁹⁸ However, our experiments revealed that particles with areas exceeding 10 mm^2 caused clog-
¹⁹⁹ ging in the feeding system and auger screw of the machine. As a result, granulometry analysis
²⁰⁰ was performed using three different mesh sizes.

²⁰¹ Figure 5 presents the obtained results, indicating that particles sifted at 5 mm exhibited
²⁰² an average area similar to the reference. There are, however, particles with areas exceeding
²⁰³ 9 mm^2 caused blockages in the feeding and extrusion section. Particles sifted to 1.5 mm
²⁰⁴ displayed a distribution ranging from 0 to approximately 3 mm^2 , which was deemed too
²⁰⁵ small for printing purposes. The presence of these small particles can lead to their complete

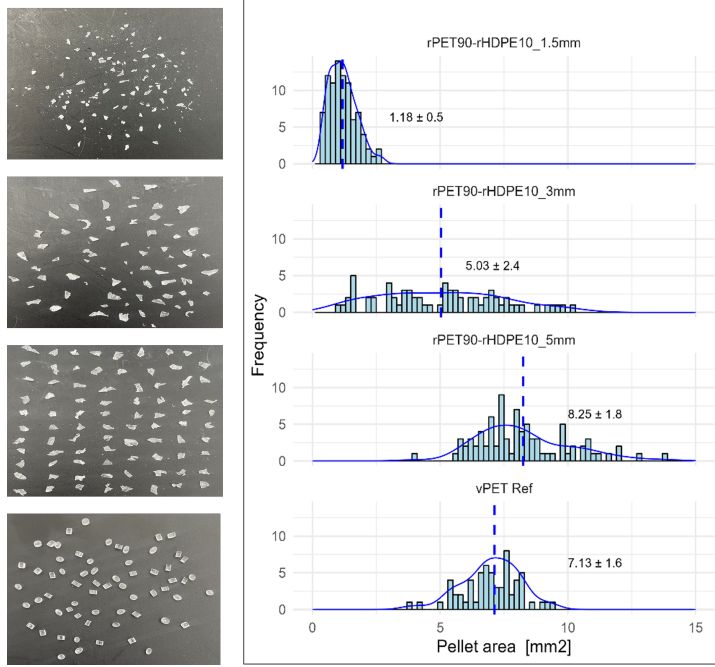


Figure 5: Granulometry analysis

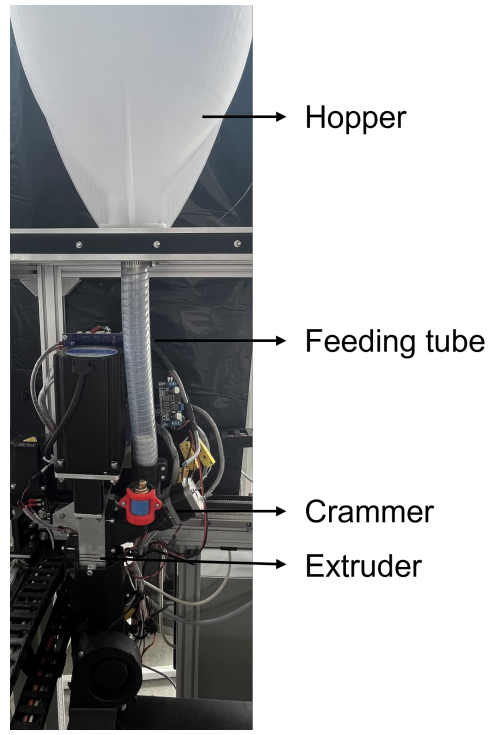


Figure 6: Gigabot feeding system

melting in the initial heat zone, thereby impeding the smooth flow of other particles and

preventing the necessary pressure for extruding the melted particles further down the screw.

Although flakes measuring 3 mm exhibited a more dispersed distribution and slightly smaller

area compared to the reference, they were found to be optimal for printing.

The final objects, however, still showed under-extrusion issues. To address this problem,

a crammer was implemented (Little et al., 2020) as presented in Figure 6. The crammer

physically pushes particles towards the auger, facilitating their transfer from the feeding

tube to the extruder. After the crammer implementation the under-extrusion issues were

greatly reduced. It was concluded that flakes with areas ranging from 1.5 mm^2 to 10 mm^2

were the most suitable for printing when using a crammer to assist the feeding system.

Chemical analysis from FTIR

Chemical structure information of the materials was obtained using FTIR spectroscopy, which

allowed the analysis of the characteristic spectral bands of the polymers.

219 In the case of rPET (bottle) four distinct bands can be observed in Figure 7. The first band,
220 located at 1713cm^{-1} represent the $C = O$ double bond. The second band, at 1240cm^{-1} ,
221 corresponds to the $C - O$ single bond ester. The third band, at 1093cm^{-1} , is associated
222 with band the methylene group and vibrations of the ester bond. Lastly, a band at 722cm^{-1}
223 which represents the CH_2 rocking bending vibration. Similar results were reported in the
224 literature for PET derived from recycled water bottles, soda bottles, and food containers
225 (Zander et al., 2018).

226 Regarding rHDPE (caps), four characteristic peaks were identified: the C-H functional group
227 bond at 2915cm^{-1} and 2847cm^{-1} , the primary bending mode of the $-\text{CH}_2$ at 1465cm^{-1}
228 and the CH_2 rocking bending vibration at 729cm^{-1} . The results obtained confirmed the
229 chemical structures of the starting materials. Additionally, no other indicative resonances,
230 apart from those associated with the polymer structures were detected. This leads to the
231 conclusion that there were no significant amounts of additives or plasticizers present in either
232 of the samples. Moreover, the spectrum of the printed blend (rPET90//rHDPE10) exhibited
233 identical characteristic peaks to those observed in the bottle, thus confirming the predominant
234 presence of PET. There are, however, noticeable differences between 1000cm^{-1} and 720cm^{-1}
235 as well as in the C-H bond (2915cm^{-1} and 2847cm^{-1} peaks), which confirm the presence of
236 HDPE (cap). The observed shift can be attributed to interactions between the two materials.

237 Thermal analysis DSC

238 The thermal properties of both recycled materials and their blend were characterized using
239 DSC to establish a baseline for optimizing process parameters of 3-D printing.

240 Two distinct endothermic peaks are observed in the representative heating and cooling ther-
241 mograms shown in Figure 8, for the printed blend sample. These peaks are associated with
242 the fusion of the crystalline fractions of rHDPE and rPET, providing confirmation of the
243 immiscibility of both materials. Moreover, the enthalpy of fusion and crystallization of the
244 rHDPE in the blend is significantly reduced, which can be attributed to the low percentage
245 of HDPE present in the blend. Furthermore, the presence of a cold crystallization peak in the

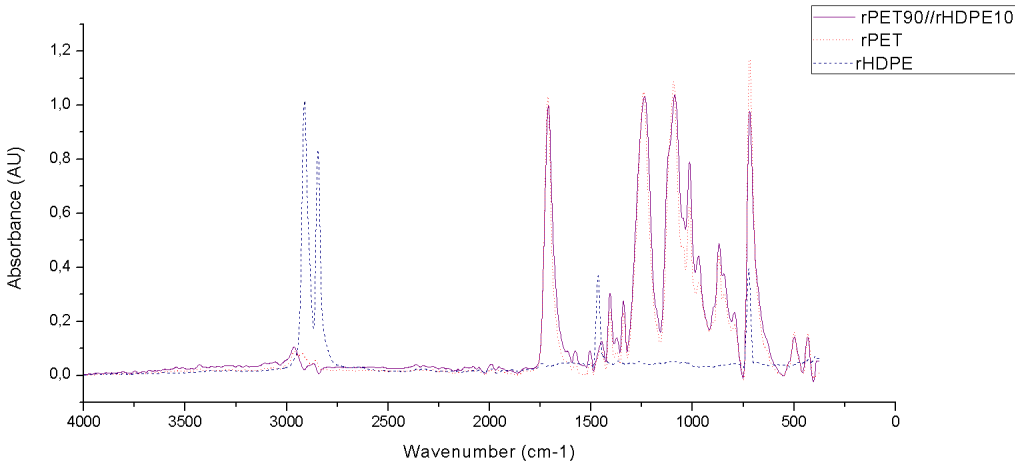
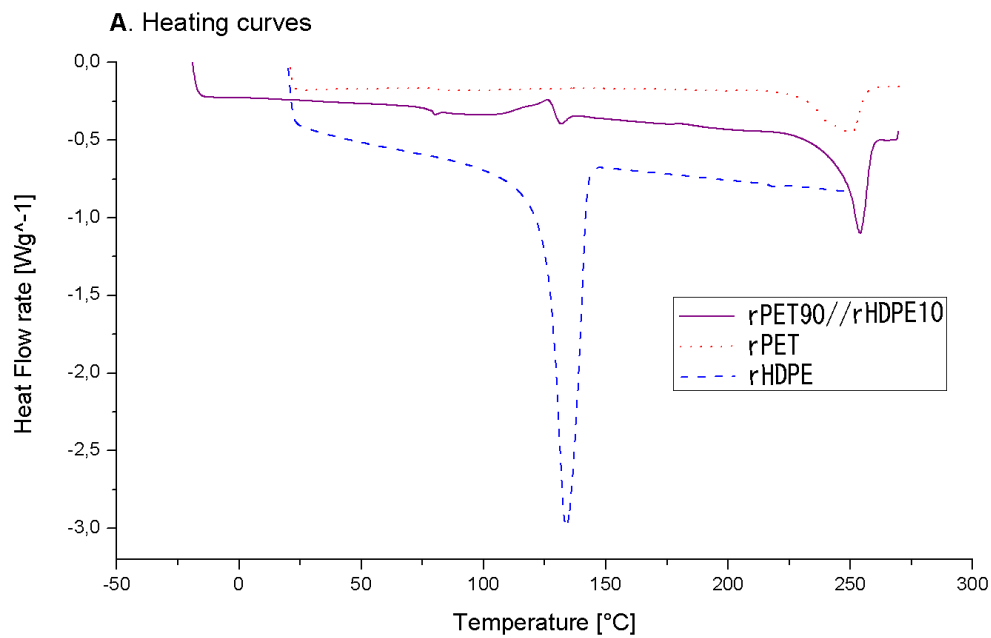


Figure 7: FTIR spectra of rPET, rHDPE, and their blend

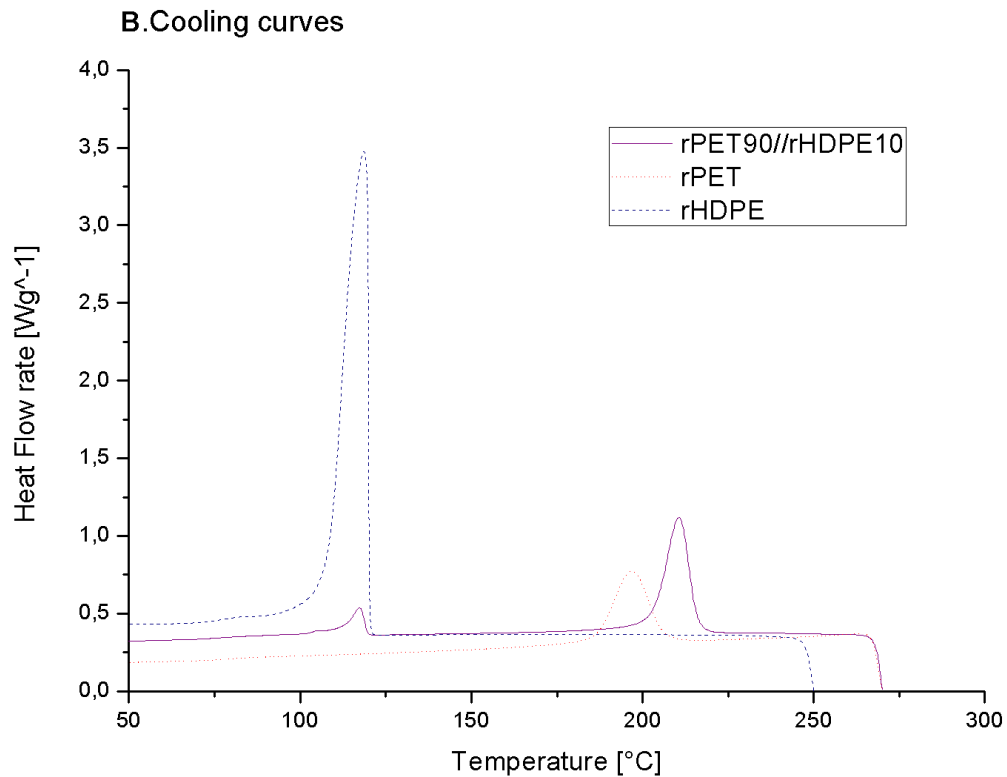
Table 2: Thermal analysis of rPET, rHDPE, and their blend

Sample	Glass transition		Melting		Crystallization		% Crystallinity Xc
	Tg (°C)		Tm (°C)	ΔHm (J/g)	Tc (°C)	ΔHc (J/g)	
rPET	82		249.9	32.3	196.7	33.3	- 23.1
rHDPE	-		133.8	172	118.7	158.2	- 58.7
rPET90/rHDPE10	77 / -		254/131.7	40.3/1.30	210.6/117.4	37.9/6.7	6.8 26.6 / 18.8

blend, but not in the individual polymers, suggests an interaction between the two polymers. It is possible that the rHDPE acts as a nucleating agent in this interaction. Table 2 lists the thermal properties of rPET, rHDPE and rPET90//rHDPE10. The melting points of rHDPE and rPET are 131.7 °C and 249.9 °C, respectively, which align with previous findings in the literature (Chen et al., 2015; Lei et al., 2009; Vaucher et al., 2022). It is observed that the melting and crystallization temperature of rPET increased, while that of rHDPE slightly decreased. Furthermore, the crystallization of rPET was found to be somewhat affected by the presence of rHDPE, resulting in a 3.5% increase in degree of crystallization. This can be attributed to the rHDPE acting as a germination point for crystallization (Vaucher et al., 2022). The slight changes in the fusion-crystallization temperatures and degree of crystallinity of rPET indicate an interaction of both polymers.



(a) Heating curves



(b) Cooling curve

Figure 8: DSC thermograms of recycled materials and blends

257 **Rheology MFI**

258 The melt flow index of the flakes was determined, enabling a fast and practical screening of the
259 viscosity of the material. Based on the DSC results, the initial temperature for the MFI test
260 was 250°C. However, the material did not flow reliably at this temperature, so it was increased
261 by 5°C to enable the determination of the melt flow index of the rPET90//rHDPE10 blend.
262 A temperature of 260°C was also tested, however, the material flowed too rapidly, making
263 difficult to obtain reliable measurements. The MFI tests were performed three times and the
264 results for the rPET90//rHDPE10 blend showed medium MFI of 39.4 ± 2.4 g/10min. This
265 value is consistent with similar values reported in the literature for rPET ([Bustos Seibert
et al., 2022; Langer et al., 2020; Nofar and Oğuz, 2019](#)). This result suggest that addition
266 of low percentage of HDPE does not significantly impact the MFI value of rPET. Since the
267 material flowed at a temperature of 255°C in the MFI test, this temperature was used as the
268 input temperature for optimizing the parameters of the 3-D printer.
269

270 **Density**

271 The density provides valuable information for estimating the cost, material usage, time con-
272 sumption, and weight of the printed object in the slicer. This information is useful to de-
273 termine the accurate printing parameters using the PSO experimenter, as the fitness of the
274 object is calculated based on its dimensional accuracy and weight. Hence, density plays a
275 significant role in determining the weight of the geometries.

276 After conducting calculations and measuring the rPET90//rHDPE10 injected object, it was
277 determined that the density of the material is 1.13 g/cm^3 . The inclusion of HDPE in the
278 matrix polymer resulted in a slight decrease in density, which is a common occurrence when
279 a polymer is mixed with a lower-density polymer. However, if we consider a PET/HDPE
280 blend with a mass ratio of 90/10, the calculated theoretical density would be 1.32 g/cm^3 . The
281 observed decrease of 14% in the results could be attributed to factors, such as experimental
282 conditions and manual measurements.

283 **Particle swarm optimization (PSO) Experimenter**

284 Geometries were 3-D printed by adjusting the parameters using the PSO Experimenter soft-
ware. The fitness function is defined by the weighted sum of the dimensional measurements
285 (length, width, height, and weight) of the printed object. A fitness value below 0.1 was con-
286 sider desirable. In the software five particles were established for each iteration, resulting in
287 five different parameter combinations being printed in each iteration.

288 After six iterations and a total of thirty lines printed, the first geometry (line) achieved a
289 fitness value of less than 0.1. The optimal parameters for this geometry are listed in column
290 two of Table 3 and images of the resulting geometries are illustrated in Figure 9 .

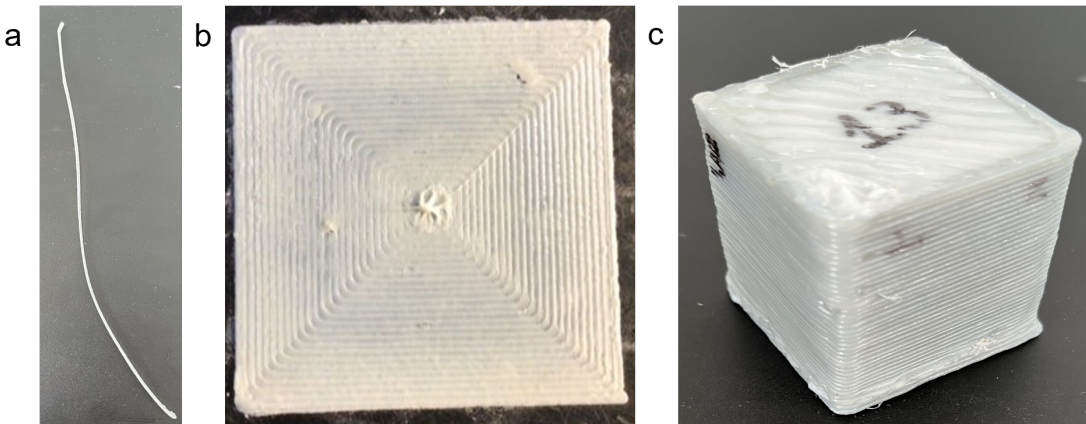


Figure 9: Images of the resulting geometries a) line, b) plane, c) cube

292 Afterwards, these parameters were used as initial guesses for plane geometry, which achieved
293 the desired fitness in the first iteration. Similarly, cubes were printed using the plane ideal
294 parameter as the initial guess, and optimal parameters, were found in the first iteration.
295 The results showed a significant decrease in printing speed, as the geometry complexity
296 increased. Moreover, the cube geometry required a higher extrusion multiplier to fill gaps and
297 overcome under-extrusion problems. The optimization of parameters for the three geometries
298 took approximately 10h reducing the experimental time, compared to conventional methods.
299 According to Oberloier et al. (2022a), this experimentation time can be reduced by 97%.
300 Indeed, the effectiveness of PSO in finding global optimum parameters is high, especially in

301 cases with a large or complex design space (Saad et al., 2019; Selvam et al., 2020).

302 Additionally, PSO converge to optimum solutions with fewer iterations than DoE meth-
303 ods (Zhang et al., 2015). Combining PSO with other meta-heuristic methods has
304 demonstrated higher ability to predict and optimize parameters (e.g. minimize surface
305 roughness(Shirmohammadi et al., 2021), compressive strength and porosity of scaffolds
306 (Asadi-Eydivand et al., 2016),and mechanical properties(Raju et al., 2019)). However, DoE
307 methods are still widely used as they provide insight into the effects of individual design
308 parameters and their interactions while the ability to find interaction between the variables
309 is not possible using PSO. In the beginning of optimization experiments, the understanding
310 the process technique and function settings might be complex. The methodology used in
311 this study, however, was easy to implement and the software used was free, open source,
312 and user-friendly, which reduced the initial difficulty. Therefore, PSO was demonstrated
313 to be an effective and highly accurate prediction technique for finding the initial optimum
314 parameters for rPET90//rHDPE10 material for FGF/FPF.

315 Based on the result, it is evident that the optimal parameters for printing may vary depending
316 on the object and each parameter has its own variation. One possible hypothesis is that the
317 geometry of the object could influence the assignment of parameters and this effect might
318 be more noticeable in large printings, yet further investigation is required to confirm this
319 hypothesis. There are several physical mechanisms at play that are expected to alter the
320 optimal printing parameters based on size and geometry of the object. For example, the
321 cooling time and temperature history of a voxel will depend on the geometry of the printed
322 object (Cleeman et al., 2022). Thus, to maintain a consisten thermal history the printing
323 parameters must be ajusted as the geometry changes. This thermal history can also have
324 more subtle effects, such as impacting the degree of crystallization even in the case of PLA
325 (Wijnen et al., 2018).

326 In addition, the effects of material extrusion are magnified with scale, including the impact of
327 thermal expansion and contraction. Small changes in contraction during cooling may cause
328 acceptable distortions for small prints, but these are magnified for larger prints (e.g. causing

Table 3: Ideal printing parameters for fused granule fabrication of waste PET and HDPE blend made from shredded whole plastic water bottles

Variable	Line value	Planes value	Cube value	Δ	Units
T1	258	263	264	6 ±3.2	°C
Tb	86	82	84	4±2	°C
Ps	21	14	10	11±5.6	mm/s
E	1.07	0.87	1.32	0.5±0.3	-

329 deformation and in the worst cases delamination or loss of bed adhesion)(Shah et al., 2019).
 330 Although, Roschli et al. (2019) showed the obstacles and possible solutions of the large-scale
 331 AM according to the way the parts are designed the incidence of the geometry in the printing
 332 parameters needs far more detailed future studies. Specifically better models for mapping
 333 3-D printing parameter optimization of small printed objects to large-volume objects are
 334 needed.

335 Functional object print

336 The final parameters for print the case study product were determined based on the ideal
 337 paraeters found for the cube geometry.However, the print speed was ajusted to decrease the
 338 printing time and prevent delamination. This adjustment was made in accordance with the
 339 PSO results, which indicated that the material can be printed at a speed range of 10 to 20
 340 mm/s. Increasing the printing speed reduces the cooling time between the layers,thereby
 341 minimizing the risk of delamination (Roschli et al., 2019), This is particularly important for
 342 larger objects, as delamination tends to be more pronounced in such cases.

343 The Gigabot X successfully produced a piece of furniture from multi-material recycled water
 344 bottles that included mixing HDPE and PET as shown in Figure 10 a.

345 The printing quality is acceptable as a prototype, proving the machine's capacity to print
 346 large-scale functional objects. The chair was able to comfortably hold a child with a mass
 347 of 20 kg, as shown in Figure 10 f. However, further evaluation is needed for the material
 348 used in the printing process. the printed object showed weak bond strength between the

adjacent layers resulting in delamination, as seen in Figure 10 b . This could be attributed to the difference in chemical properties of the materials, their immiscibility (Chu et al., 2022; William et al., 2021), high crystallinity (Verma et al., 2023) and the large volume of the object as delamination issues were more prominent during the printing of the chair compared to the parameters optimization process. The delamination observed in larger objects can be attributed to the rapid cooling of the layers before the material is once again deposited. This is in contrast to cube printing, where the smaller surface area allows better layer adhesion before complete cooling. Even popular 3-D printing materials like PLA can be affected by this issue, as observed from the print surface (Wijnen et al., 2018). To address the delamination problem and improve material properties, the addition of agents that reduce could be beneficial (Dai et al., 1997; Inoya et al., 2012; Kramer et al., 1994). This can enhance interfacial bonds through polymer modification (Gao et al., 2021) and viscosity reduction (Ko et al., 2019). Additionally, we observed printing warping problems (Figure 10 c), which are likely caused by the high crystallization rates of HDPE (Schirmeister et al., 2019). We tested the use of Magigoo adhesive (Thought3D Ltd., Paola, Malta) and the addition of a brim to improve bed adhesion, yet these solutions did not completely resolve the problem. A previous study showed that the use of a building plate made of thermoplastic elastomer SEBS allowed the adhesion of the plastic and facilitated easy detachment of the printed object without any breakage or damage [(schirmeister2019.This?) suggests a potential solution that should be further evaluated in future work. Another visible issue present in the close angles of the printed object was the shrinkage (Figure 10 d) which occurs during solidification and particularly upon polymer crystallization. Moreover, it is well-known that PET has hygroscopic tendencies and easily absorbs moisture from the temperature, which makes it difficult to extrude (Bustos Seibert et al., 2022). As a result, it is likely to break down in the presence of water, lowering the quality of the print. Prior to printing the chair some samples exhibited brittle behavior and void formation therefore, the material was consistently dried and the hopper was kept closed to prevent moisture from entering the environment. These measures helped to ensure a more suitable material for printing. Additionally, there are visible vibration and ringing problems (Figure 10 e) caused by the machine upgrades. Both acceleration and

378 jerk (the maximum value of instantaneous speed change) require finer tuning to resolve these
379 issues.

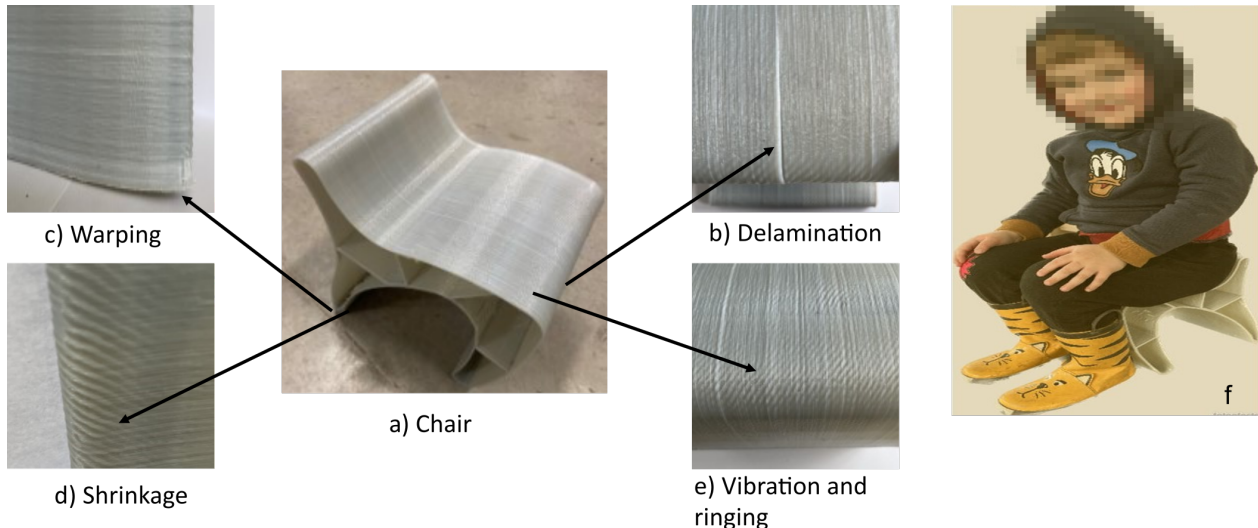


Figure 10: Finished children's chair and printing issues

380 Cost and environmental impact

381 The printing process took 10 hours and the printed object weighs 840 grams. Due to the
382 found optimized speed being low, the printing rate (grams per hour) is low considering the
383 machine that pellet printers have a typical throughput of 220 g to 9 kg per hour. To improve
384 the printing time, upgrading the the extruder motor to a more powerful would be beneficial.
385 Besides, the energy required for 10 hours of 3-D printing was found to be 6 kW-hr resulting in
386 a production cost of ~1.2 € in function of the electricity cost in France, and does not include
387 the material cost, as the bottles used were obtained from post-consumer waste. When labor
388 costs are not included, the price was significant reduced (~88%) compared to the low-cost
389 options available in the market.

390 The economics of fabricating the case study product remained competitive even when using
391 recycled plastic pellets or shreds, which are available on the market for prices ranging from 1-
392 10 €/kg. However, it is important to note that labor, maintenance, and machine devaluation
393 were not considered in the final price. These factors should be considered in future work to

394 ensure a comprehensive economic evaluation.

395 Regarding the environmental impact, this study does not evaluate the entire life cycle of
396 the printed object. However, various scientific studies have already shown the feasibility of
397 distributed recycling (Kerdlap et al., 2022; Santander et al., 2020). A comparison between
398 conventional and distributed manufacturing in terms of energy consumption and emissions
399 has been conducted (Kreiger and Pearce, 2013). Other studies have examined the environ-
400 mental performance of AM (Colorado et al., 2020; Garcia et al., 2018) and the appearance
401 of DRAM as a source of raw material for diverse 3-D printers coming from post-consumer
402 plastic waste in the form of either filament (Hart et al., 2018; Mikula et al., 2021; Mohammed
403 et al., 2017b; Pakkanen et al., 2017b) or granules (Alexandre et al., 2020).

404 Additionally, Caceres-Mendoza et al. (2023) have developed a comprehensive life cycle assess-
405 ment of a DRAM system focusing on the production of PLA filament, comparing virgin and
406 recycled materials. The findings of their environmental analysis revealed a analysis revealed
407 a reduction of approximately 97% in the production impacts, including climate change, fossil
408 depletion, water depletion, and potential eutrophication, when using recycled filament as op-
409 posed to virgin filament. It is important to note that these results are subject to the energy
410 supply and might vary depending on the geographical location.

411 Conclusion and future work

412 This study examined the feasibility of using mixed post-consumer waste as a feedstock mate-
413 rial for direct 3-D printing without the need of compatibilization. The results demostrated
414 the potential of mixing solid waste plastics (PET/HDPE) to be used as feedstock material,
415 as evidenced by successfully printing a water bottle using two incompatible polymers from
416 the cap and body of the bottle. Additionally, the results found that a large-scale FGF 3-D
417 printer was capable of producing cost-effective functional object using these mixed waste
418 PET/HDPE plastics. However, further research is necessary to analyze the mechanical prop-
419 erties of the material and explore the use of compatibilizers that can enhance the interphase

420 tension between plastics and reduce their crystallinity. These measures could potentially
421 improve and enhance the properties of both the material and the 3-D printed parts.

422 These considerations become increasingly important as the size of the 3-D printed part in-
423 creases. The improvement of the material science of this approach can also offer an opportu-
424 nity to improve the quality of the printing time, reduce energy consumption of the machine,
425 and improve the economic viability of DRAM using mixed plastic waste.

426 In addition, future work could assess the different combinations or blends of commodity
427 plastics with or without the use of compatibilizers, to determine their printability. This
428 investigation could lead to the elimination of the selection/sorting process. In the same way,
429 the development of a methodology that ensures process reproducibility, even in areas with
430 limited infrastructure opens up the potential for plastic revalorization using DRAM.

431 **Declaration of competing**

432 The authors declare that they have no known competing financial interests or personal rela-
433 tionships that could have appeared to influence the work reported in this paper.

434 **Acknowledgments**

435 This project has received funding from the European Union's Horizon 2020 research and
436 innovation program under grant agreement No 869952. The authors thank the LUE program
437 for the financing of the thesis, the Lorraine Fab Living lab platform and the Thompson
438 endowment.

439 **References**

- 440 Alexandre, A., Cruz Sanchez, F.A., Boudaoud, H., Camargo, M., Pearce, J.M., 2020. Me-
441 chanical Properties of Direct Waste Printing of Polylactic Acid with Universal Pellets
442 Extruder: Comparison to Fused Filament Fabrication on Open-Source Desktop Three-
443 Dimensional Printers. *3D Printing and Additive Manufacturing* 7, 237–247. <https://doi.org/10.1089/3dp.2019.0195>
- 445 Anderson, I., 2017. Mechanical Properties of Specimens 3D Printed with Virgin and Recycled
446 Polylactic Acid. *3D Printing and Additive Manufacturing* 4, 110–115. <https://doi.org/10.1089/3dp.2016.0054>
- 448 Asadi-Eydivand, M., Solati-Hashjin, M., Fathi, A., Padashi, M., Abu Osman, N.A., 2016.
449 Optimal design of a 3D-printed scaffold using intelligent evolutionary algorithms. *Applied
450 Soft Computing* 39, 36–47. <https://doi.org/10.1016/j.asoc.2015.11.011>
- 451 Attaran, M., 2020. 3D Printing Role in Filling the Critical Gap in the Medical Supply Chain
452 during COVID-19 Pandemic. *American Journal of Industrial and Business Management*
453 10, 988–1001. <https://doi.org/10.4236/ajibm.2020.105066>
- 454 Baechler, C., DeVuono, M., Pearce, J.M., 2013. Distributed recycling of waste polymer into
455 RepRap feedstock. *Rapid Prototyping Journal* 19, 118–125. <https://doi.org/10.1108/13552541311302978>
- 457 Bowyer, A., 2014. 3D Printing and Humanity's First Imperfect Replicator. *3D Printing and
458 Additive Manufacturing* 1, 4–5. <https://doi.org/10.1089/3dp.2013.0003>
- 459 Bustos Seibert, M., Mazzei Capote, G.A., Gruber, M., Volk, W., Osswald, T.A., 2022. Man-
460 ufacturing of a PET Filament from Recycled Material for Material Extrusion (MEX).
461 *Recycling* 7, 69. <https://doi.org/10.3390/recycling7050069>
- 462 Byard, D.J., Woern, A.L., Oakley, R.B., Fiedler, M.J., Snabes, S.L., Pearce, J.M., 2019.
463 Green fab lab applications of large-area waste polymer-based additive manufacturing.
464 *Additive Manufacturing* 27, 515–525. <https://doi.org/10.1016/j.addma.2019.03.006>
- 465 Caceres-Mendoza, C., Santander-Tapia, P., Cruz Sanchez, F.A., Troussier, N., Camargo,
466 M., Boudaoud, H., 2023. Life cycle assessment of filament production in distributed
467 plastic recycling via additive manufacturing. *Cleaner Waste Systems* 5, 100100. <https://doi.org/10.1016/j.clwas.2023.100100>
- 469 Carrete, I.A., Quiñonez, P.A., Bermudez, D., Roberson, D.A., 2021. Incorporating Textile-
470 Derived Cellulose Fibers for the Strengthening of Recycled Polyethylene Terephthalate
471 for 3D Printing Feedstock Materials. *Journal of polymers and the environment*.
- 472 Chen, R.S., Ab Ghani, M.H., Salleh, M.N., Ahmad, S., Tarawneh, M.A., 2015. Mechanical,
473 water absorption, and morphology of recycled polymer blend rice husk flour biocomposites.
474 *Journal of Applied Polymer Science* 132. <https://doi.org/10.1002/app.41494>
- 475 Chong, S., Pan, G.-T., Khalid, M., Yang, T.C.-K., Hung, S.-T., Huang, C.-M., 2017. Physi-
476 cal Characterization and Pre-assessment of Recycled High-Density Polyethylene as 3D

- 477 Printing Material. *Journal of Polymers and the Environment* 25, 136–145. <https://doi.org/10.1007/s10924-016-0793-4>
- 478
- 479 Choong, Y.Y.C., Tan, H.W., Patel, D.C., Choong, W.T.N., Chen, C.-H., Low, H.Y., Tan, M.J., Patel, C.D., Chua, C.K., 2020. The global rise of 3D printing during the COVID-19 pandemic. *Nat Rev Mater* 5, 637–639. <https://doi.org/10.1038/s41578-020-00234-3>
- 480
- 481
- 482 Chu, J.S., Koay, S.C., Chan, M.Y., Choo, H.L., Ong, T.K., 2022. Recycled plastic filament made from post-consumer expanded polystyrene and polypropylene for fused filament fabrication. *Polymer Engineering & Science* 62, 3786–3795. <https://doi.org/10.1002/pen.26144>
- 483
- 484
- 485
- 486 Cleeman, J., Bogut, A., Mangrolia, B., Ripberger, A., Kate, K., Zou, Q., Malhotra, R., 2022. Scalable, Flexible and Resilient Parallelization of Fused Filament Fabrication: Breaking Endemic Tradeoffs in Material Extrusion Additive Manufacturing. *Additive Manufacturing* 102926. <https://doi.org/10.1016/J.ADDMA.2022.102926>
- 487
- 488
- 489
- 490 Colorado, H.A., Velásquez, E.I.G., Monteiro, S.N., 2020. Sustainability of additive manufacturing: The circular economy of materials and environmental perspectives. *Journal of Materials Research and Technology* 9, 8221–8234. <https://doi.org/10.1016/j.jmrt.2020.04.062>
- 491
- 492
- 493
- 494 Corsini, L., Aranda-Jan, C.B., Moultrie, J., 2022. The impact of 3D printing on the humanitarian supply chain. <https://doi.org/10.17863/CAM.51226>
- 495
- 496 Cruz Sanchez, F.A., Boudaoud, H., Camargo, M., Pearce, J.M., 2020. Plastic recycling in additive manufacturing: A systematic literature review and opportunities for the circular economy. *Journal of Cleaner Production* 264, 121602. <https://doi.org/10.1016/j.jclepro.2020.121602>
- 497
- 498
- 499
- 500 Cruz Sanchez, F.A., Boudaoud, H., Hoppe, S., Camargo, M., 2017. Polymer recycling in an open-source additive manufacturing context: Mechanical issues. *Additive Manufacturing* 17, 87–105. <https://doi.org/10.1016/j.addma.2017.05.013>
- 501
- 502
- 503 Dai, C.-A., Jandt, K.D., Iyengar, D.R., Slack, N.L., Dai, K.H., Davidson, W.B., Kramer, E.J., Hui, C.-Y., 1997. Strengthening Polymer Interfaces with Triblock Copolymers. *Macromolecules* 30, 549–560. <https://doi.org/10.1021/ma960396s>
- 504
- 505
- 506 Dertinger, S.C., Gallup, N., Tanikella, N.G., Grasso, M., Vahid, S., Foot, P.J.S., Pearce, J.M., 2020. Technical pathways for distributed recycling of polymer composites for distributed manufacturing: Windshield wiper blades. *Resources, Conservation and Recycling* 157, 104810. <https://doi.org/10.1016/j.resconrec.2020.104810>
- 507
- 508
- 509
- 510 Despeisse, M., Baumers, M., Brown, P., Charnley, F., Ford, S.J., Garmulewicz, A., Knowles, S., Minshall, T.H.W., Mortara, L., Reed-Tsochas, F.P., Rowley, J., 2017. Unlocking value for a circular economy through 3D printing: A research agenda. *Technological Forecasting and Social Change* 115, 75–84. <https://doi.org/10.1016/j.techfore.2016.09.021>
- 511
- 512
- 513
- 514 Evode, N., Qamar, S.A., Bilal, M., Barceló, D., Iqbal, H.M.N., 2021. Plastic waste and its management strategies for environmental sustainability. *Case Studies in Chemical and*
- 515

- 516 Environmental Engineering 4, 100142. <https://doi.org/10.1016/j.cscee.2021.100142>
- 517 Fontana, L., Giubilini, A., Arrigo, R., Malucelli, G., Minetola, P., 2022. Characterization
518 of 3D Printed Polylactic Acid by Fused Granular Fabrication through Printing Accuracy,
519 Porosity, Thermal and Mechanical Analyses. Polymers 14, 3530. <https://doi.org/10.3390/polym14173530>
- 520
- 521 Ford, S., Despesse, M., 2016. Additive manufacturing and sustainability: An exploratory
522 study of the advantages and challenges. Journal of Cleaner Production 137, 1573–1587.
523 <https://doi.org/10.1016/j.jclepro.2016.04.150>
- 524 Gaikwad, V., Ghose, A., Cholake, S., Rawal, A., Iwato, M., Sahajwalla, V., 2018. Transforma-
525 tion of E-Waste Plastics into Sustainable Filaments for 3D Printing. ACS Sustainable
526 Chemistry & Engineering 6, 14432–14440. <https://doi.org/10.1021/acssuschemeng.8b03105>
- 527
- 528 Gallup, N., Bow, J.K., Pearce, J.M., 2018. Economic Potential for Distributed Manufacturing
529 of Adaptive Aids for Arthritis Patients in the U.S. Geriatrics 3, 89. <https://doi.org/10.3390/geriatrics3040089>
- 530
- 531 Gao, X., Qi, S., Kuang, X., Su, Y., Li, J., Wang, D., 2021. Fused filament fabrication
532 of polymer materials: A review of interlayer bond. Additive Manufacturing 37, 101658.
533 <https://doi.org/10.1016/j.addma.2020.101658>
- 534 Garcia, F.L., Moris, V.A. da S., Nunes, A.O., Silva, D.A.L., 2018. Environmental perfor-
535 mance of additive manufacturing process – an overview. Rapid Prototyping Journal 24,
536 1166–1177. <https://doi.org/10.1108/RPJ-05-2017-0108>
- 537 Geyer, R., 2020. Chapter 2 - Production, use, and fate of synthetic polymers, in: Letcher,
538 T.M. (Ed.), Plastic Waste and Recycling. Academic Press, pp. 13–32. <https://doi.org/10.1016/B978-0-12-817880-5.00002-5>
- 539
- 540 Geyer, R., Jambeck, J.R., Law, K.L., 2017. Production, use, and fate of all plastics ever
541 made. Science Advances 3, e1700782. <https://doi.org/10.1126/sciadv.1700782>
- 542 Grassi, G., Spagnolo, S.L., Paoletti, I., 2019. Fabrication and durability testing of a 3D
543 printed façade for desert climates. Additive Manufacturing 28, 439.
- 544 Gwamuri, J., Franco, D., Khan, K.Y., Gauchia, L., Pearce, J.M., 2016. High-Efficiency Solar-
545 Powered 3-D Printers for Sustainable Development. Machines 4, 3. <https://doi.org/10.3390/machines4010003>
- 546
- 547 Hart, K.R., Frketic, J.B., Brown, J.R., 2018. Recycling meal-ready-to-eat (MRE) pouches
548 into polymer filament for material extrusion additive manufacturing. Additive Manufac-
549 turing 21, 536–543. <https://doi.org/10.1016/j.addma.2018.04.011>
- 550 ImageJ, 2023. Image processing and analysis in java [WWW Document]. URL <https://imagej.nih.gov/ij/download.html> (accessed 6.13.2023).
- 551
- 552 Inoya, H., Wei Leong, Y., Klinklai, W., Thumsorn, S., Makata, Y., Hamada, H., 2012. Compatibilization of recycled poly (ethylene terephthalate) and polypropylene blends:
553 Effect of polypropylene molecular weight on homogeneity and compatibility. Journal of
- 554

- 555 applied polymer science 124, 3947–3955.
- 556 Jaisingh Sheoran, A., Kumar, H., 2020. Fused Deposition modeling process parameters optimiza-
557 tion and effect on mechanical properties and part quality: Review and reflection on
558 present research. Materials Today: Proceedings, International Conference on Mechanical
559 and Energy Technologies 21, 1659–1672. <https://doi.org/10.1016/j.matpr.2019.11.296>
- 560 Jonathan GUIDIGO1, Stéphane MOLINA2, Edmond C. ADJOVI3, André MERLIN
561 4, DONNOT André5, Merlin SIMO TAGNE6, 2017. Polyethylene Low and High
562 Density-Polyethylene Terephthalate and Polypropylene Blend as Matrices for Wood
563 Flour, in: International Journal of Science and Research (IJSR). pp. 1069–1074.
564 <https://doi.org/10.21275/ART20164296>
- 565 Jones, R., Haufe, P., Sells, E., Iravani, P., Olliver, V., Palmer, C., Bowyer, A., 2011. RepRap
566 – the replicating rapid prototyper. Robotica 29, 177–191. <https://doi.org/10.1017/S026>
567 357471000069X
- 568 Kerdlap, P., Purnama, A.R., Low, J.S.C., Tan, D.Z.L., Barlow, C.Y., Ramakrishna, S.,
569 2022. Comparing the environmental performance of distributed versus centralized plastic
570 recycling systems: Applying hybrid simulation modeling to life cycle assessment. Journal
571 of Industrial Ecology 26, 252–271. <https://doi.org/10.1111/jiec.13151>
- 572 King, D., Babasola, A., Rozario, J., Pearce, J., 2014. Mobile Open-Source Solar-Powered
573 3-D Printers for Distributed Manufacturing in Off-Grid Communities. Challenges in
574 Sustainability 2. <https://doi.org/10.12924/cis2014.02010018>
- 575 Ko, Y.S., Herrmann, D., Tolar, O., Elspass, W.J., Brändli, C., 2019. Improving the filament
576 weld-strength of fused filament fabrication products through improved interdiffusion. Add-
577 tive Manufacturing 29, 100815. <https://doi.org/10.1016/j.addma.2019.100815>
- 578 Kramer, E.J., Norton, L.J., Dai, C.-A., Sha, Y., Hui, C.-Y., 1994. Strengthening polymer
579 interfaces. Faraday Discussions 98, 31–46. <https://doi.org/10.1039/FD9949800031>
- 580 Kratofil, L., Hrnjak-Murgić, Z., Jelencć, J., Andrićć, B., Kovacé, T., Merzel, V., 2006. Study
581 of the compatibilizer effect on blends prepared from waste poly (ethylene-terephthalate)
582 and high density polyethylene. International Polymer Processing 21, 328–335.
- 583 Kreiger, M.A., Mulder, M.L., Glover, A.G., Pearce, J.M., 2014. Life cycle analysis of dis-
584 tributed recycling of post-consumer high density polyethylene for 3-D printing filament.
585 Journal of Cleaner Production 70, 90–96. <https://doi.org/10.1016/j.jclepro.2014.02.009>
- 586 Kreiger, M., Pearce, J.M., 2013. Environmental Impacts of Distributed Manufacturing from
587 3-D Printing of Polymer Components and Products. MRS Proceedings 1492, 85–90.
588 <https://doi.org/10.1557/opl.2013.319>
- 589 Langer, E., Bortel, K., Waskiewicz, S., Lenartowicz-Klik, M., 2020. Methods of PET Recy-
590 cling, Plasticizers Derived from Post-Consumer PET. <https://doi.org/10.1016/b978-0->
591 [323-46200-6.00005-2](https://doi.org/10.1016/b978-0-323-46200-6.00005-2)
- 592 Lei, Y., Wu, Q., Zhang, Q., 2009. Morphology and properties of microfibrillar composites
593 based on recycled poly (ethylene terephthalate) and high density polyethylene. Compos-

- 594 ites Part A: Applied Science and Manufacturing 40, 904–912. <https://doi.org/10.1016/j.compositesa.2009.04.017>
- 595
- 596 Lipsky, S., Przyjemska, A., Velasquez, M., Gershenson, J., 2019. 3D Printing for Humanitarian Relief: The Printer Problem, in: 2019 IEEE Global Humanitarian Technology Conference (GHTC). pp. 1–7. <https://doi.org/10.1109/GHTC46095.2019.9033053>
- 597
- 598
- 599 Little, H.A., Tanikella, N.G., J. Reich, M., Fiedler, M.J., Snabes, S.L., Pearce, J.M., 2020. 600 Towards Distributed Recycling with Additive Manufacturing of PET Flake Feedstocks. 601 Materials 13, 4273. <https://doi.org/10.3390/ma13194273>
- 602
- 603 Löschke, S.K., Mai, J., Proust, G., Brambilla, A., 2019. Microtimber: The Development of 604 a 3D Printed Composite Panel Made from Waste Wood and Recycled Plastics. Digital 605 Wood Design 24, 827–848. https://doi.org/10.1007/978-3-030-03676-8_33
- 606
- 607 MacArthur, E., 2017. Beyond plastic waste. Science 358, 843–843. <https://doi.org/10.1126/science.aa06749>
- 608
- 609 Mikula, K., Skrzypczak, D., Izydorczyk, G., Warchoł, J., Moustakas, K., Chojnacka, K., 610 Witek-Krowiak, A., 2021. 3D printing filament as a second life of waste plastics—a review. Environmental Science and Pollution Research 28, 12321–12333. <https://doi.org/10.1007/s11356-020-10657-8>
- 611
- 612 Mohammed, M.I., Das, A., Gomez-Kervin, E., Wilson, D., Gibson, I., 2017a. EcoPrinting: 613 Investigating the Use of 100% Recycled Acrylonitrile Butadiene Styrene (ABS) for Additive Manufacturing. University of Texas at Austin.
- 614
- 615 Mohammed, M.I., Mohan, M., Das, A., Johnson, M.D., Badwal, P.S., McLean, D., Gibson, I., 616 2017b. A low carbon footprint approach to the reconstitution of plastics into 3D-printer 617 filament for enhanced waste reduction. KnE Engineering 234–241. <https://doi.org/10.18502/keg.v2i2.621>
- 618
- 619 Mohammed, M.I., Wilson, D., Gomez-Kervin, E., Rosson, L., Long, J., 2018. EcoPrinting: 620 Investigation of Solar Powered Plastic Recycling and Additive Manufacturing for Enhanced 621 Waste Management and Sustainable Manufacturing, in: 2018 IEEE Conference on 622 Technologies for Sustainability (SusTech). IEEE, pp. 1–6. <https://doi.org/10.1109/SusTech.2018.8671370>
- 623
- 624 Nofar, M., Oğuz, H., 2019. Development of PBT/Recycled-PET Blends and the Influence 625 of Using Chain Extender. Journal of Polymers and the Environment 27, 1404–1417. 626 <https://doi.org/10.1007/s10924-019-01435-w>
- 627
- 628 Novak, J.I., Loy, J., 2020. A critical review of initial 3D printed products responding to COVID-19 health and supply chain challenges. Emerald Open Research 2, 24. <https://doi.org/10.35241/emeraldopenres.13697.1>
- 629
- 630 Oberloier, S., Whisman, N.G., Pearce, J.M., 2022a. Finding Ideal Parameters for Recycled 631 Material Fused Particle Fabrication-Based 3D Printing Using an Open Source Software 632 Implementation of Particle Swarm Optimization. 3D Printing and Additive Manufacturing. <https://doi.org/10.1089/3dp.2022.0012>

- 633 Oberloier, S., Whisman, N.G., Pearce, J.M., 2022b. Finding Ideal Parameters for Recycled
634 Material Fused Particle Fabrication-Based 3D Printing Using an Open Source Software
635 Implementation of Particle Swarm Optimization. *3D Printing and Additive Manufactur-*
636 *ing*. <https://doi.org/10.1089/3dp.2022.0012>
- 637 Pakkanen, J., Manfredi, D., Minetola, P., Iuliano, L., 2017a. About the Use of Recycled or
638 Biodegradable Filaments for Sustainability of 3D Printing, in: Campana, G., Howlett,
639 R.J., Setchi, R., Cimatti, B. (Eds.), Springer International Publishing, Cham, pp. 776–
640 785. https://doi.org/10.1007/978-3-319-57078-5_73
- 641 Pakkanen, J., Manfredi, D., Minetola, P., Iuliano, L., 2017b. About the Use of Recycled or
642 Biodegradable Filaments for Sustainability of 3D Printing, in: Campana, G., Howlett,
643 R.J., Setchi, R., Cimatti, B. (Eds.), *Sustainable Design and Manufacturing 2017, Smart*
644 *Innovation, Systems and Technologies*. Springer International Publishing, Cham, pp.
645 776–785. https://doi.org/10.1007/978-3-319-57078-5_73
- 646 Pan, Y., Wu, G., Ma, H., Zhou, S., Zhang, H., 2020. Improved compatibility of PET/HDPE
647 blend by using GMA grafted thermoplastic elastomer. *Polymer-Plastics Technology and*
648 *Materials* 59, 1887–1898.
- 649 Pearce, J., Qian, J.-Y., 2022. Economic Impact of DIY Home Manufacturing of Consumer
650 Products with Low-cost 3D Printing from Free and Open Source Designs. *European*
651 *Journal of Social Impact and Circular Economy* 3, 1–24. <https://doi.org/10.13135/2704-9906/6508>
- 653 Petersen, E., Kidd, R., Pearce, J., 2017. Impact of DIY Home Manufacturing with 3D
654 Printing on the Toy and Game Market. *Technologies* 5, 45. <https://doi.org/10.3390/te-chnologies5030045>
- 656 Petsiuk, A., Lavu, B., Dick, R., Pearce, J.M., 2022. Waste Plastic Direct Extrusion Hang-
657 printer. *Inventions* 7, 70. <https://doi.org/10.3390/inventions7030070>
- 658 Pringle, A.M., Rudnicki, M., Pearce, J.M., 2018. Wood Furniture Waste-Based Recycled 3-D
659 Printing Filament. *Forest Products Journal* 68, 86–95. <https://doi.org/10.13073/FPJ-D-17-00042>
- 661 Raju, M., Gupta, M.K., Bhanot, N., Sharma, V.S., 2019. A hybrid PSO–BFO evolutionary
662 algorithm for optimization of fused deposition modelling process parameters. *Journal of*
663 *Intelligent Manufacturing* 30, 2743–2758. <https://doi.org/10.1007/s10845-018-1420-0>
- 664 Rattan, R.S., Nauta, N., Romani, A., Pearce, J.M., 2023. Hangprinter for large scale additive
665 manufacturing using fused particle fabrication with recycled plastic and continuous
666 feeding. *HardwareX* 13, e00401. <https://doi.org/10.1016/j.hwx.2023.e00401>
- 667 Reich, M.J., Woern, A.L., Tanikella, N.G., Pearce, J.M., 2019. Mechanical Properties and
668 Applications of Recycled Polycarbonate Particle Material Extrusion-Based Additive Man-
669 ufacturing. *Materials* 12, 1642. <https://doi.org/10.3390/ma12101642>
- 670 Rett, J.P., Traore, Y.L., Ho, E.A., 2021. Sustainable Materials for Fused Deposition Modeling
671 3D Printing Applications. *Advanced Engineering Materials* 23, 2001472. <https://doi.or>

- 672 [g/10.1002/adem.202001472](https://doi.org/10.1002/adem.202001472)
- 673 Romani, A., Rognoli, V., Levi, M., 2021. Design, Materials, and Extrusion-Based Additive
674 Manufacturing in Circular Economy Contexts: From Waste to New Products. Sustainability
675 13, 7269. <https://doi.org/10.3390/su13137269>
- 676 Roschli, A., Gaul, K.T., Boulger, A.M., Post, B.K., Chesser, P.C., Love, L.J., Blue, F., Borish,
677 M., 2019. Designing for Big Area Additive Manufacturing. Additive Manufacturing 25,
678 275–285. <https://doi.org/10.1016/j.addma.2018.11.006>
- 679 Saad, M.S., Nor, A.M., Baharudin, M.E., Zakaria, M.Z., Aimani, A.F., 2019. Optimization of
680 surface roughness in FDM 3D printer using response surface methodology, particle swarm
681 optimization, and symbiotic organism search algorithms. The International Journal of
682 Advanced Manufacturing Technology 105, 5121–5137. <https://doi.org/10.1007/s00170-019-04568-3>
- 683 Salmi, M., Akmal, J.S., Pei, E., Wolff, J., Jaribion, A., Khajavi, S.H., 2020. 3D Printing
684 in COVID-19: Productivity Estimation of the Most Promising Open Source Solutions in
685 Emergency Situations. Applied Sciences 10, 4004. <https://doi.org/10.3390/app10114004>
- 686 Santander, P., Cruz Sanchez, F.A., Boudaoud, H., Camargo, M., 2020. Closed loop supply
687 chain network for local and distributed plastic recycling for 3D printing: A MILP-based
688 optimization approach. Resources, Conservation and Recycling 154, 104531. <https://doi.org/10.1016/j.resconrec.2019.104531>
- 689 Savonen, B.L., Mahan, T.J., Curtis, M.W., Schreier, J.W., Gershenson, J.K., Pearce, J.M.,
690 2018. Development of a Resilient 3-D Printer for Humanitarian Crisis Response. Technologies
691 6, 30. <https://doi.org/10.3390/technologies6010030>
- 692 Schirmeister, C.G., Hees, T., Licht, E.H., Mülhaupt, R., 2019. 3D printing of high density
693 polyethylene by fused filament fabrication. Additive Manufacturing 28, 152–159. <https://doi.org/10.1016/j.addma.2019.05.003>
- 694 Sells, E., Smith, Z., Bailard, S., Bowyer, A., Olliver, V., 2009. RepRap: The Replicating
695 Rapid Prototyper - maximizing customizability by breeding the means of production,
696 in: Piller, F.T., Tseng, M.M. (Eds.), Handbook of Research in Mass Customization and
697 Personalization. World Scientific, pp. 568–580.
- 698 Selvam, A., Mayilswamy, S., Whenish, R., 2020. Strength Improvement of Additive Manufac-
699 turing Components by Reinforcing Carbon Fiber and by Employing Bioinspired Interlock
700 Sutures. Journal of Vinyl and Additive Technology 26, 511–523. <https://doi.org/10.1002/vnl.21766>
- 701 Shah, J., Snider, B., Clarke, T., Kozutsky, S., Lacki, M., Hosseini, A., 2019. Large-scale
702 3D printers for additive manufacturing: Design considerations and challenges. The
703 International Journal of Advanced Manufacturing Technology 104, 3679–3693. <https://doi.org/10.1007/s00170-019-04074-6>
- 704 Shirmohammadi, M., Goushchi, S.J., Keshtiban, P.M., 2021. Optimization of 3D printing
705 process parameters to minimize surface roughness with hybrid artificial neural network

- 711 model and particle swarm algorithm. *Progress in Additive Manufacturing* 6, 199–215.
712 <https://doi.org/10.1007/s40964-021-00166-6>
- 713 Siltaloppi, J., Jähi, M., 2021. Toward a sustainable plastics value chain: Core conundrums
714 and emerging solution mechanisms for a systemic transition. *Journal of Cleaner Production*
715 315, 128113. <https://doi.org/10.1016/j.jclepro.2021.128113>
- 716 Soares, J., Miguel, I., Venâncio, C., Lopes, I., Oliveira, M., 2021. Public views on plastic
717 pollution: Knowledge, perceived impacts, and pro-environmental behaviours. *Journal of*
718 *Hazardous Materials* 412, 125227. <https://doi.org/10.1016/j.jhazmat.2021.125227>
- 719 Taghavi, S.K., Shahrajabian, H., Hosseini, H.M., 2018. Detailed comparison of compatibi-
720 lizers MAPE and SEBS-g-MA on the mechanical/thermal properties, and morphology
721 in ternary blend of recycled PET/HDPE/MAPE and recycled PET/HDPE/SEBS-g-MA.
722 *Journal of Elastomers & Plastics* 50, 13–35.
- 723 Van de Voorde, B., Katalagarianakis, A., Huysman, S., Toncheva, A., Raquez, J.-M., Duretek,
724 I., Holzer, C., Cardon, L., Bernaerts, K., V, Van Hemelrijck, D., Pyl, L., Van Vlierberghe,
725 S., 2022. Effect of extrusion and fused filament fabrication processing parameters of recy-
726 cled poly(ethylene terephthalate) on the crystallinity and mechanical properties. *Additive*
727 *Manufacturing* 50. <https://doi.org/10.1016/j.addma.2021.102518>
- 728 Vaucher, J., Demongeot, A., Michaud, V., Leterrier, Y., 2022. Recycling of Bottle Grade
729 PET: Influence of HDPE Contamination on the Microstructure and Mechanical Perfor-
730 mance of 3D Printed Parts. *Polymers* 14, 5507. <https://doi.org/10.3390/polym14245507>
- 731 Verma, N., Awasthi, P., Gupta, A., Banerjee, S.S., 2023. Fused Deposition Modeling of
732 Polyolefins: Challenges and Opportunities. *Macromolecular Materials and Engineering*
733 308, 2200421. <https://doi.org/10.1002/mame.202200421>
- 734 Wijnen, B., Sanders, P., Pearce, J.M., 2018. Improved model and experimental validation
735 of deformation in fused filament fabrication of polylactic acid. *Progress in Additive*
736 *Manufacturing* 3, 193–203. <https://doi.org/10.1007/s40964-018-0052-4>
- 737 William, L.J.W., Koay, S.C., Chan, M.Y., Pang, M.M., Ong, T.K., Tshai, K.Y., 2021.
738 Recycling Polymer Blend made from Post-used Styrofoam and Polypropylene for Fuse
739 Deposition Modelling. *Journal of Physics: Conference Series* 2120, 012020. <https://doi.org/10.1088/1742-6596/2120/1/012020>
- 741 Woern, A.L., McCaslin, J.R., Pringle, A.M., Pearce, J.M., 2018. RepRapable Recyclebot:
742 Open source 3-D printable extruder for converting plastic to 3-D printing filament. *Hard-
743 wareX* 4, e00026. <https://doi.org/10.1016/j.ohx.2018.e00026>
- 744 Wong, J.Y., 2015. Ultra-Portable Solar-Powered 3D Printers for Onsite Manufacturing of
745 Medical Resources. *Aerospace Medicine and Human Performance* 86, 830–834. <https://doi.org/10.3357/AMHP.4308.2015>
- 747 Zander, N.E., Gillan, M., Burckhard, Z., Gardea, F., 2019. Recycled polypropylene blends
748 as novel 3D printing materials. *Additive Manufacturing* 25, 122–130. <https://doi.org/10.1016/j.addma.2018.11.009>

- 750 Zander, N.E., Gillan, M., Lambeth, R.H., 2018. Recycled polyethylene terephthalate as a
751 new FFF feedstock material. Additive Manufacturing 21, 174–182. <https://doi.org/10.1016/j.addma.2018.03.007>
- 753 Zhang, Y., Wang, S., Ji, G., 2015. A Comprehensive Survey on Particle Swarm Optimization
754 Algorithm and Its Applications. Mathematical Problems in Engineering 2015, e931256.
755 <https://doi.org/10.1155/2015/931256>
- 756 Zhong, S., Pearce, J.M., 2018. Tightening the loop on the circular economy: Coupled dis-
757 tributed recycling and manufacturing with recyclebot and RepRap 3-D printing. Re-
758 sources, Conservation and Recycling 128, 48–58. <https://doi.org/10.1016/j.resconrec.2017.09.023>
- 759